Modeling of impurity effect on drift instabilities in plasmas with many ion species

S. Moradi, M. Z. Tokar, and B. Weyssow

Citation: Physics of Plasmas **17**, 012101 (2010); doi: 10.1063/1.3283390
View online: https://doi.org/10.1063/1.3283390
View Table of Contents: http://aip.scitation.org/toc/php/17/1
Published by the American Institute of Physics

Modeling of impurity effect on drift instabilities in plasmas with many ion species

S. Moradi,[1,a)] M. Z. Tokar,[2] and B. Weyssow[3,b)]
[1]*Department of Statistical and Plasma Physics, Universite Libre de Bruxelles, 1050 Brussels, Belgium*
[2]*Institute für Energieforschung-Plasmaphysik, Forschungszentrum Jülich, Association EURATOM-FZJ, Trilateral Euregio Cluster, 52425 Jülich, Germany*
[3]*EFDA-CSU, D-85748 Garching, München, Germany*

(Received 25 August 2009; accepted 10 December 2009; published online 6 January 2010)

Drift microinstabilities, being the main cause of anomalous transport of charged particles and energy in fusion plasmas, can be strongly influenced by the presence of impurities. Normally a large amount of different ion species from diverse charge states and chemical elements is present. An approach, providing a possibility to take into account an arbitrary number of ion species in analysis of instabilities, is proposed and applied to study the impurity effect on unstable modes due to ion temperature gradient and trapped electrons described in a linear fluid approximation. The method is validated by comparing with the results from direct calculations in a one impurity ion case. The dependence of instability characteristics and anomalous transport coefficients on the absolute level and radial gradient of impurity density is investigated. Plasmas with several impurity ion species, including C^{+6}, N^{+7}, O^{+8}, Ne^{+10}, and Ar^{+18} whose density peaking factors are determined self-consistently from the impurity zero flux condition, are considered as an example of applications. [doi:10.1063/1.3283390]

I. INTRODUCTION

It is well known that anomalous transport in hot fusion plasmas can be significantly influenced by impurities. Experiments performed on several fusion devices demonstrated that a significant modification of particles and energy losses can be achieved with deliberate seeding of noble gases both in the low (L) and high (H) confinement modes.[1–5] It is believed that such a behavior originated in the impact of impurities on drift microinstabilities, being the main cause of anomalous transport, and several theoretical approaches have been proposed to explain these effects.[6–12] In studies cited above, an effective impurity ion is normally introduced, in spite of the fact that a large number of different ion species from diverse charge states of different elements is present in real fusion plasmas. Already the definition of the charge and mass of an effective impurity ion is not straightforward in such a case. However, the main uncertainty is emerging by characterizing the density gradient of an effective impurity species; experimental observations show that the density profiles are qualitatively different for different impurities, tending to be hollow in the case of light species like carbon and significantly peaked for heavy impurities like nickel.[13] Since the impurity density gradient essentially affects the instability characteristics, the impact of impurity can be studied firmly by considering realistic plasmas if all ion species are individually taking into account.

The inclusion of any additional species increases the number of transport equations involved in analysis, at least by three those describing the density, temperature, and parallel velocity perturbations, see, e.g., Refs. 14 and 15. By a standard treatment this complicates essentially the procedure for the derivation of the dispersion equation for the frequency of unstable modes in a polynomial form which is normally used. Also the order of this equation increases and the reliability of its numerical solution deteriorates. In the present paper we develop a method to solve the dispersion equation with contributions from arbitrary number of impurity species. Within this approach the effect of impurity is taken into account in an iterative procedure starting with the solution of the dispersion equation where the impurity contribution is neglected completely. The instability characteristics found in this approximation are used by calculating the response in impurity parameters to the fluctuation of electrostatic potential. This approximate response is employed then in the dispersion equation with the impurity effects included. The found solution is used to refine the impurity response and the procedure is repeated until the convergence is reached. The method proposed is validated by comparing with the results of direct calculations in the case of one impurity ion species. It is also applied to study the impurity effect in plasmas with many ion species on unstable modes due to ion temperature gradient (ITG) and trapped electron considered in a linear fluid approximation. The modification of instability characteristics, such as the growth rates, real frequencies, and wave number of most unstable modes, and anomalous transport coefficients with the impurity concentration, is investigated. The density gradients of impurity ions are determined self-consistently from the condition of zero particle flux.

a)Electronic mail: smoradi@ulb.ac.be.
b)Also at Department of Statistical and Plasma Physics, Universite Libre de Bruxelles, Brussels, Belgium.

II. BASIC EQUATIONS

Each ion species j, including main plasma ions and impurity, with the charge Z_j and mass m_j is described by the continuity, parallel momentum, and energy transport equations for its density n_j, parallel velocity $V_{\|j}$, and temperature T_j:

$$\frac{\partial n_j}{\partial t} + \nabla \cdot (n_j \mathbf{V}_j) = 0, \tag{1}$$

$$m_j n_j \frac{dV_{\|j}}{dt} + \nabla_\| (n_j T_j) + Z_j n_j e \nabla_\| \varphi = 0, \tag{2}$$

$$\frac{3}{2} n_j \frac{dT_j}{dt} - T_j \frac{\partial n_j}{\partial t} + \nabla \cdot \mathbf{q}_j - T_j \mathbf{V}_j \cdot \nabla n_j = 0, \tag{3}$$

where $\mathbf{V}_j$ is the sum of the parallel velocity and the perpendicular drift velocity, $\mathbf{V}_{\perp j}$; the latter arises due to the electric field $\mathbf{E}=-\nabla\varphi$, pressure gradient, inertia force, and viscosity responsible for finite-Larmor-radius (FLR) effects;[16] φ is the electrostatic potential, and the convective derivative is defined as $d/dt=\partial/\partial t+\mathbf{V}_j\cdot\nabla$; $\mathbf{q}_j=2.5n_jT_j[\mathbf{B}\times\nabla T_j]/(Z_jeB^2)$ is the diamagnetic drift heat flux[17] with the magnetic field $\mathbf{B}$ dependent on the poloidal angle ϑ, $B=B_0/(1+r\cos\vartheta/R)$, with r and R being the minor and major radii of the magnetic surface.

The electron plasma component is separated on trapped and freely circulating particles. For the former the bounce averaged parallel velocity is zero and the density n_{et} and temperature T_{et} are described by continuity and energy conservation equations:

$$\frac{\partial n_{et}}{\partial t} + \nabla \cdot (n_{et} \mathbf{V}_{\perp e}) = S_{t,f}, \tag{4}$$

$$\frac{3}{2} n_{et} \frac{dT_{et}}{dt} - T_{et} \frac{\partial n_{et}}{\partial t} + \nabla \cdot \mathbf{q}_{et} - T_{et} \mathbf{V}_{\perp e} \cdot \nabla n_{et} = Q_{t,f}, \tag{5}$$

where the drift velocity $\mathbf{V}_{\perp e}$ is calculated by neglecting FLR effects and inertia effects; $\mathbf{q}_{et}=2.5n_{et}T_{et}[\mathbf{B}\times\nabla T_{et}]/(eB^2)$; the terms $S_{t,f}$ and $Q_{t,f}$, providing the particle and energy exchange between trapped and freely circulating electrons due to Coulomb collisions, are taken into account according to Ref. 18. Parallel mass velocity of freely circulating electrons is much smaller that their thermal one and inertia can be neglected in the force balance along magnetic field where the pressure gradient is balanced by the electric force,

$$\nabla_\| (T_{ef} n_{ef}) = e n_{ef} \nabla_\| \varphi. \tag{6}$$

In a stationary state all particle densities and temperatures are assumed to be functions of the minor radius r only; parallel velocities of the ions and the electrostatic potential are zero. The plasma quasineutrality requires

$$n_i + \sum_{j\neq i} Z_j n_j = n_e = n_{et} + n_{ef} \tag{7}$$

with the fractions of trapped electrons, $f_{et}\equiv n_{et}/n_e$, equal to $\sqrt{2r/(r+R)}$. The temperatures of trapped and freely circulating electrons are assumed the same, $T_{et}=T_{ef}\equiv T_e$.

Consider small perturbations of parameters, varying in time with a complex frequency ω, and spatially, along the magnetic field, direction l, and on the magnetic surface perpendicular to the field lines, direction y, with the wave numbers $k_\|$ and k_y, respectively, $\delta f \sim \exp(-i\omega t + ik_\| l + ik_y y)$. By linearizing the transport Eqs. (1)–(3) we get[14,15]

$$\left(\bar{\omega} + \frac{\lambda\tau_j}{Z_j}\right)\tilde{n}_j - \lambda(\epsilon_{n_j} - 1)\tilde{\varphi} + \frac{\lambda\tau_j}{Z_j}\tilde{T}_j + \frac{m_j}{Z_j m_i} k_\perp^2 \rho_s^2 \left[\bar{\omega} + \frac{\lambda\tau_j}{Z_j}(\epsilon_{n_j} + \epsilon_{T_j})\right]\tilde{\varphi} - \tilde{V}_{\|j} = 0, \tag{8}$$

$$\left(\bar{\omega} - 2\frac{\lambda\tau_j}{Z_j}\right)\tilde{V}_{\|j} - \xi\frac{Z_j m_i}{m_j}\tilde{\varphi} - \tau_j \xi \frac{m_i}{m_j}(\tilde{T}_j + \tilde{n}_j) = 0, \tag{9}$$

$$\left(\bar{\omega} + \frac{5}{3}\frac{\lambda\tau_j}{Z_j}\right)\tilde{T}_j - \lambda\left(\epsilon_{T_j} - \frac{2}{3}\epsilon_{n_j}\right)\tilde{\varphi} - \frac{2}{3}\bar{\omega}\tilde{n}_j = 0, \tag{10}$$

where the dimensionless fluctuations $\tilde{n}_j=\delta n_j/n_j$, $\tilde{T}_j=\delta T_j/T_j$, $\tilde{\varphi}=e\delta\varphi/T_e$, and $\tilde{V}_{\|j}=k_\|\delta V_{\|j}/\omega_{D_e}$ have been introduced, $\bar{\omega}=\omega/\omega_{De}$ with the magnetic drift frequency $\omega_{De}=2k_yT_e/(eBR)$, $\epsilon_x=-d\ln x/dr\times R/2$ are the dimensionless radial gradients of stationary parameters, $\xi=[Rk_\|/(2k_y\rho_s)]^2$, $\rho_s=c_s/\omega_{Li}$ is the ion Larmor radius with $c_s=\sqrt{T_e/m_i}$ being the ion sound speed, and ω_{Li} the main ion Larmor frequency; $\tau_j=T_j/T_e$. By following Ref. 19 the values θ-averaged over the assumed perturbation eigenfunction[20] are assumed for the components of the mode wave vector, $k_\|=1/\sqrt{3}/(q_{sf}R)$ and $k_\perp=k_y\sqrt{1+(\pi^2/3-5/2)s^2}$, where q_{sf} is the safety factor and $s=(r/q_{sf})dq_{sf}/dr$ the magnetic shear. The corresponding averaging of ω_{De} results in the factor $\lambda=2/3+s\cdot 5/9$. A strong ballooning approximation with the eigenfunction independent of the magnetic shear, applied in Ref. 19, is not valid for large and small values of s. Therefore our results concerning the magnetic shear effect on characteristics of instabilities and anomalous impurity transport have to be checked in the future by applying a more adequate approach.

The linearization of Eqs. (4) and (5) for trapped electrons results in

$$(\bar{\omega} - \lambda_t)\tilde{n}_{et} - \lambda_t(\epsilon_{n_e} - 1)\tilde{\varphi} - \lambda_t\tilde{T}_{et} = \bar{\nu}_{th}(\Gamma\tilde{\varphi} - \tilde{n}_{et}), \tag{11}$$

$$\left(\bar{\omega} - \tfrac{5}{3}\lambda_t\right)\tilde{T}_{et} - \lambda_t\left(\epsilon_{T_e} - \tfrac{2}{3}\epsilon_{n_e}\right)\tilde{\varphi} - \tfrac{2}{3}\bar{\omega}\tilde{n}_{et} = \bar{\nu}_{th}(\tilde{n}_{et} + \beta\tilde{\varphi}), \tag{12}$$

where $\lambda_t=1/4+2s/3$ arises by bounce averaging,[19] $\bar{\nu}_{th}=R\nu_{ei}/(r\omega_{D_e})$ with ν_{ei} being the frequency of electron collisions with ions, $\Gamma=1+(\epsilon_{T_e}/\epsilon_{n_e})[\omega_{*e}/(\omega-\omega_{D_e}+i\nu_{th})]$, $\beta=1.5-2.5\Gamma$.[18] Perturbations in the temperature of freely circulating electrons are neglected because of high parallel heat conduction; therefore the Boltzmann relation follows from Eq. (6), $\tilde{n}_{ef}=\tilde{\varphi}$.

III. SOLUTION OF DISPERSION EQUATION

The sets of linearized Eqs. (8)–(12) allow to express the perturbations of the densities of ion species and trapped electrons through the perturbation of the electrostatic potential, $\tilde{n}_j = P_j \tilde{\varphi}$ and $\tilde{n}_{et} = P_{et} \tilde{\varphi}$, respectively. The coefficients P_j and P_{et} are given in the Appendix. Together with the Boltzmann relation for freely circulating electrons these expressions can be substituted into the quasineutrality condition providing a dispersion relation for the perturbation frequency ω,

$$P_i\left(1 - \sum_{j \neq i} Z_j \xi_j\right) + \sum_{j \neq i} P_j Z_j \xi_j = P_{et} f_{et} + 1 - f_{et}. \tag{13}$$

Here the contribution from the main plasma ions with $j=i$ is separated explicitly and the concentrations of impurity ions $\xi_j \equiv n_j / n_e$ are introduced.

In order to use standard subroutines by solving the dispersion Eq. (13) it has to be reduced to a polynomial form. The inclusion of any new impurity species into consideration makes the derivation of this equation more troublesome and increases its order by 3, thus making its numerical solution less reliable. For this reason another approach based on a treatment of the impurity contribution, the second term on left hand side in Eq. (13), by iterations has been applied. This procedure begins with solving of Eq. (13) with the impurity contribution neglected completely, i.e., with $\xi_{j \neq i} = 0$. The solution ω found in this way is used to calculate approximate values of the coefficients $P_{j \neq i}$. Then Eq. (13) is solved with the approximate impurity contribution calculated with actual $\xi_{j \neq i} \neq 0$ and the described procedure is continued until the convergence is reached. This method allows us to analyze the effect on plasma instabilities from arbitrary number of impurity species, e.g., with all charge states of carbon, nitrogen, oxygen, neon, argon, etc.

In order to validate the proposed approach we compare the results of calculations for one impurity species with those obtained when the contribution from impurity has been taken into account explicitly. Figure 1 shows such a comparison for the dependences of the instability growth rate $\gamma \equiv \mathrm{Im}\ \omega$ on the dimensionless perpendicular wave number $k_y \rho_s$ calculated for 3% concentration of Ne^{+10} impurity ions for three magnitudes of $\epsilon_{T_i} = \epsilon_{T_e}$, with $\epsilon_{n_{e,i}} = 5$ and $\epsilon_{n_{\mathrm{Ne}}} = 0$. Other parameters are taken from JET experiments dedicated to impurity transport studies, see Ref. 21, at $r/a = 0.8$: $T_i = T_e = 1$ keV, $n_e = 2.5 \times 10^{19}$ m^{-3}, $q_{sf} = 4$, and $s = 1.8$. Since the dispersion Eq. (13) has several solutions the one with the largest growth rate $\gamma > 0$ is selected for each $k_y \rho_s$. There is a very good agreement between both approaches.

By applying the single impurity ion method while considering real plasmas with a large number of impurity species from diverse charge states of different elements, one has to introduce the mass, charge, density, and density gradient of the effective impurity species. Already the former three parameters can be defined in different ways, affecting the results. However, the most uncertain point is the introduction of the density gradient for the effective impurity ion since experimental observations show that the density profiles are qualitatively different for different impurities. They tend to be hollow in the case of light species like carbon and significantly peaked for heavy impurities like nickel.[13] Thus, there is no guarantee that the density gradient of the effective impurity ion mimics the real situation. Figures 2 and 3 show for the case of a single impurity species Ne^{+10} that the results are, however, very sensitive to the dimensionless density gradient. In the left column of Fig. 2 the maximum value of γ, $\gamma_{\max}$, is shown for the range of $0.05 < k_y \rho_s < 1$ as a function of $\epsilon_{T_{e,i}}$ computed for different values of the neon concentration ξ_{Ne} and density gradient scale $\epsilon_{n_{\mathrm{Ne}}}$. In the middle and right columns the real frequency part $\omega_r = \mathrm{Re}\ \omega$ and the dimensionless wave vector $k_y \rho_s$ of the most unstable modes are, respectively, displayed. In all cases, $\omega_r < 0$, i.e., the modes are driven by the ITGs. Practically always the growth rate decreases with increasing impurity concentration. For $\epsilon_{T_{e,i}} \geq 7.5$ the behavior is qualitatively similar for different $\epsilon_{n_{\mathrm{Ne}}}$, however, the quantitate difference to the reference case without impurity becomes significant for large impurity con-

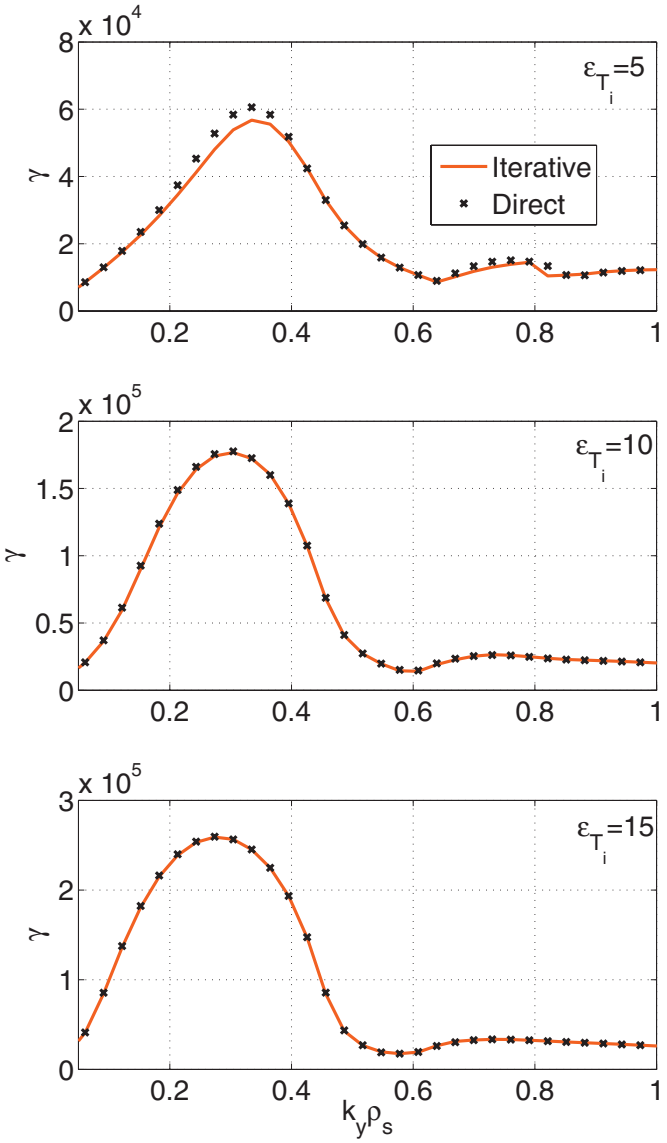

FIG. 1. (Color) The $k_y \rho_s$-spectra of ITG/TE instability growth rate in deuterium plasma containing 3% of Ne^{10+} ions with a flat density profile, $\epsilon_{n_{\mathrm{Ne}}} = 0$, calculated directly in a one impurity species approximation (symbols) and iteratively (solid lines).

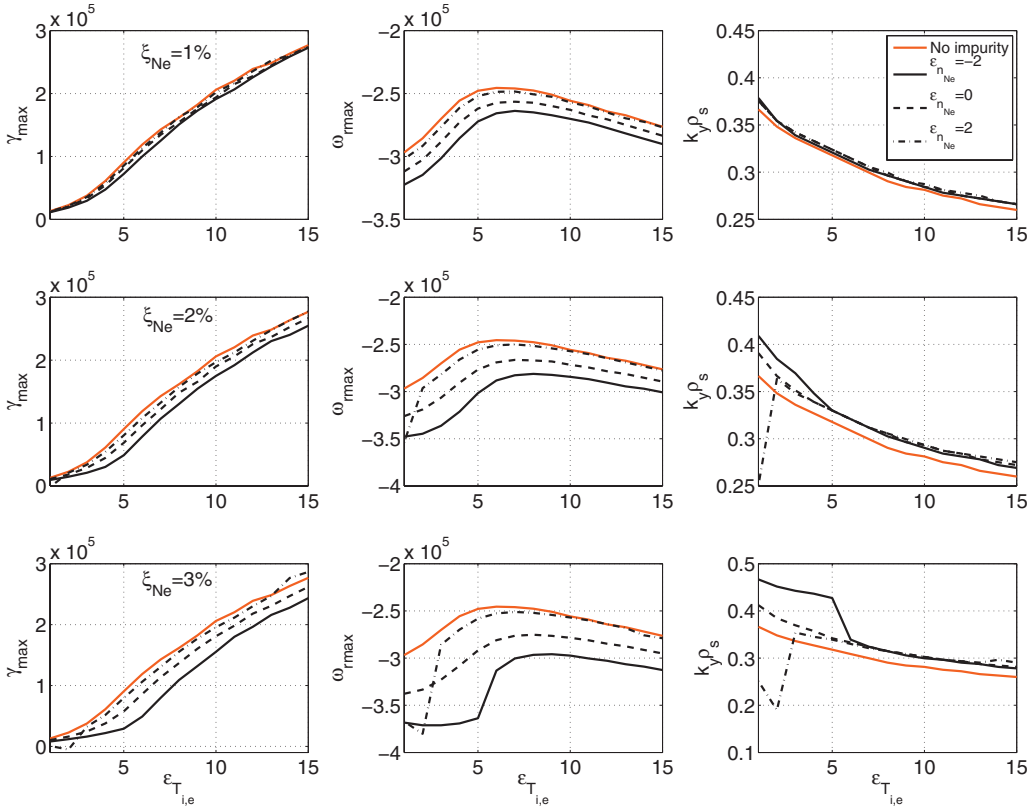

FIG. 2. (Color) The growth rates (left column), real frequency (middle column), and dimensionless wave vector (right column) of the most unstable modes as functions of the temperature gradient parameter $\epsilon_{T_{e,i}}$ calculated with different concentrations ξ_{Ne} and density gradient parameters $\epsilon_{n_{\mathrm{Ne}}}$ of Ne^{10+} impurity ions.

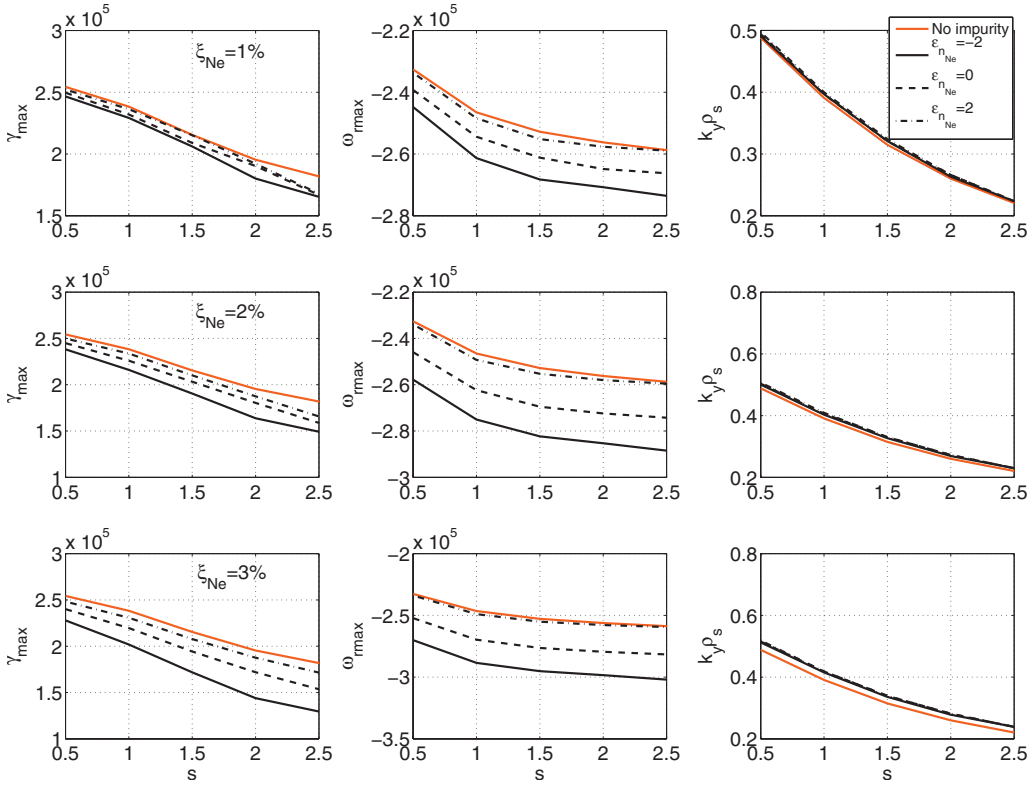

FIG. 3. (Color) The growth rates (left column), real frequency (middle column), and dimensionless wave vector (right column) as functions of magnetic shear calculated for different concentrations ξ_{Ne} and density gradient parameters $\epsilon_{n_{\mathrm{Ne}}}$ of neon impurity.

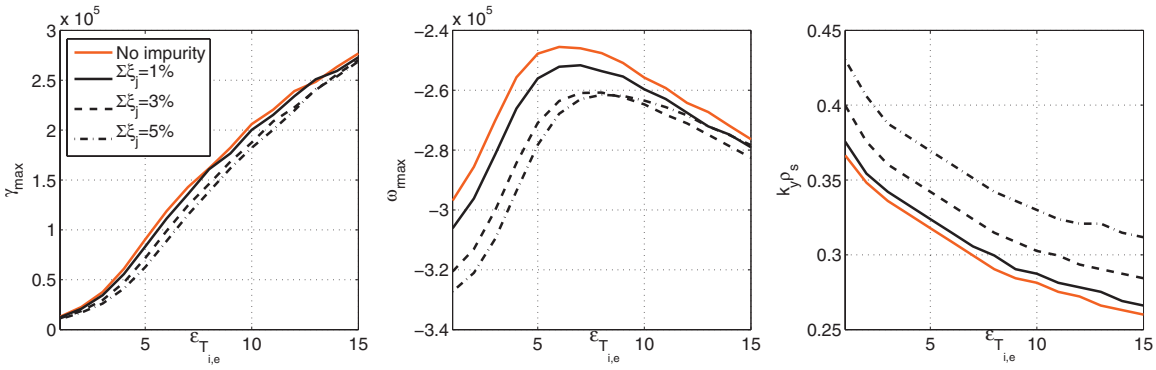

FIG. 4. (Color) The growth rates (left column), real frequency (middle column), and dimensionless wave vector (right column) vs temperature gradient scale in deuterium plasma with C^{+6}, N^{+7}, O^{+8}, Ne^{+10}, and Ar^{+18} impurity ions of different total concentrations: no impurity (red curves), $\Sigma\xi_j=1\%$ (black solid curves), 3% (black dashed curves), and 5% (black dashed-dotted curves); the impurity ion density gradient parameters are calculated self-consistently from zero particle fluxes.

centration. For most unstable modes $k_y\rho_s \approx 0.3$, i.e., close to the value typical for ITG mode due to main deuterium ions.[16] For smaller $\epsilon_{T_{e,i}}$ the deviations from the reference case are larger, especially for nonflat density profiles with $\epsilon_{n_{\mathrm{Ne}}} \neq 0$. For the peaked n_{Ne} profile with $\epsilon_{n_{\mathrm{Ne}}}=2$ a new impurity driven mode with significantly reduced $k_y\rho_s$ exists at $\epsilon_{T_{e,i}} \leq 2.5$. Since the growth rate does not change too much compared to the reference case without impurity, we have to expect an increase in the transport characteristics, e.g., the particle diffusion as $1/k_x^2$. For a hollow neon density profile with $\epsilon_{n_{\mathrm{Ne}}}=-2$ another impurity driven mode starts to dominate if $\epsilon_{T_{e,i}} \leq 5$, with significantly reduced growth rate and wavelength compared to the reference situation. Therefore a reduction in transport has to be expected. The found behavior describes a self-stabilizing effect of impurities on transport at small temperature gradients; an increased impurity transport by peaked impurity density will presumably prevent peaking and vice versa. Therefore it is important to calculate the impurity density gradient represented by the parameter ϵ_{n_j} in a self-consistent way as it will be done in the next section by considering plasmas with several impurity species. Figure 3 displays the same characteristics as functions of magnetic shear, s.

The results above show that at high enough impurity concentration the instability characteristics are sensitive, in particular, to the impurity density gradient. In plasmas with several impurity species characterized by very different gradients it is, however, fully unclear how to define the density gradient for such an effective impurity species. Therefore a reliable approach to treat instabilities with all ion species taken individually into account is of importance.

IV. TRANSPORT COEFFICIENTS

The effect of impurities on the characteristics of ITG/TE unstable modes is mimicked also in the behavior of transport coefficients. These can be assessed from the definitions of anomalous fluxes of particles and heat, see Appendix and Ref. 16. Thus, for the particle flux density, $\Gamma_{e,j}$, one gets

$$\Gamma_{e,j} = -2n_{et,j}\frac{T_e k_y}{eB}|\tilde{\varphi}|^2 \mathrm{Im}(P_{et,j}). \tag{14}$$

In the factors $P_{et,j}$ one can distinguish the parts proportional to $\epsilon_{n_{et,j}}$ and independent of this, i.e., $P_{et,j}=P_{De,j}\epsilon_{n_{e,j}}+P_{Ve,j}$. As a result Γ_j is separated into diffusive and convective parts proportional, correspondingly, to the density gradient and density itself, $\Gamma_{e,j}=-D_{e,j}(\partial n_{e,j}/\partial r)+V_{e,j}n_{e,j}$. Here

$$D_{e,j} = -\frac{T_e k_y R}{eB}|\tilde{\varphi}|^2 \mathrm{Im}(P_{De,j}),$$
$$V_{e,j} = -\frac{2T_e k_y}{eB}|\tilde{\varphi}|^2 \mathrm{Im}(P_{Ve,j}), \tag{15}$$

are the diffusivities and convective velocities. The absolute level of the transport coefficients is governed by the amplitude of the potential perturbation. Without nonlinear turbulence simulations this can be only roughly estimated in mixing length approximation, see, e.g., Ref. 16, $|\tilde{\varphi}| \sim \gamma_{\max}/(k_y^2\rho_s c_s)$.

The impurity density profiles are usually characterized by the peaking factor $p_j \equiv -R\nabla_r n_j/n_j = 2\epsilon_{n_j}$.[13] In a steady state the fluxes of impurity ions reduce to zero and from the definitions above one gets $p_j=-RV_j/D_j=-2\ \mathrm{Im}\ P_{Vj}/\mathrm{Im}\ P_{Dj}$, i.e., a value independent of $|\tilde{\varphi}|$. This allows to determine p_j and ϵ_{n_j}, which is involved in the dispersion equation, in an iterative procedure. Namely, such a self-consistent approach is applied henceforth by considering mixtures of five completely stripped impurity ion species C^{+6}, N^{+7}, O^{+8}, Ne^{+10}, and Ar^{+18}. The contributions of individual species to the total impurity concentration are defined by adopting the same contributions $Z_j n_j$ to the electron density n_e. Figures 4 and 5 show the linear growth rate and real frequency of the most unstable modes and Figs. 6 and 7, the transport coefficients $D_{e,i}$ and $V_{e,i}$, as functions of the plasma temperature gradient parameter $\epsilon_{T_{i,e}}$ and magnetic shear s. As one can see, the increase in impurity concentration leads normally to a decrease in the particle diffusivities and absolute values of their convective velocities caused by the reduction in the growth rate of unstable modes. Figures 8 and 9 show the impurity

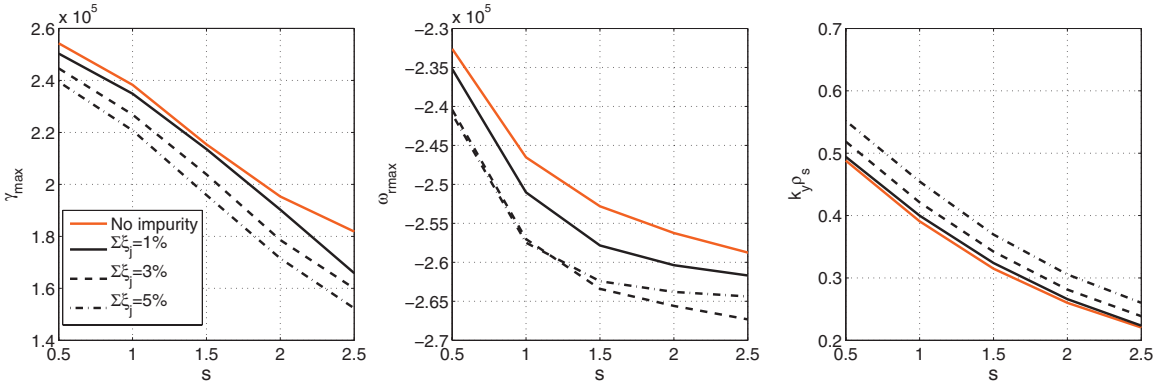

FIG. 5. (Color) The growth rates (left column), real frequency (middle column), and dimensionless wave vector (right column) vs magnetic shear computed for $\epsilon_{T_{e,i}}=10$.

peaking factor, p, for C^{+6}, Ne^{+10}, and Ar^{+18} impurity ions. In these calculations the ITG-dominated situation with $\epsilon_{T_e}=0$ and $R/L_{n_e}=3$ has been considered in order to compare with previous studies. In agreement with Ref. 12 the peaking factor is an increasing function of the ion charge Z for low impurity concentrations with $\Sigma\xi_j=1\%$. This tendency, however, vanishes at higher impurity concentrations if either the ITG is not too large or the magnetic shear is not too small.

Similarly to the particle fluxes one can calculate anomalous heat fluxes. With the relations between perturbations of the temperatures and electrostatic potential, $\tilde{T}_{et,j}=Q_{et,j}\tilde{\varphi}$, found from linearized transport Eqs. (8)–(12), one gets for the heat flux contributions nonvanishing for zero particle fluxes,

$$q_{e,j}=-2n_{et,j}\frac{T_e k_y}{eB}|\tilde{\varphi}|^2\mathrm{Im}(Q_{et,j}). \tag{16}$$

Also the factors $Q_{et,j}$ can be separated in parts, correspondingly, proportional and independent of the temperature gradients, $Q_{et,j}=Q^{\nabla T}_{et,j}\epsilon_{T_{et,j}}+Q^{T}_{et,j}$, see Appendix. Therefore the heat flux densities also have conductive and pinch contributions,

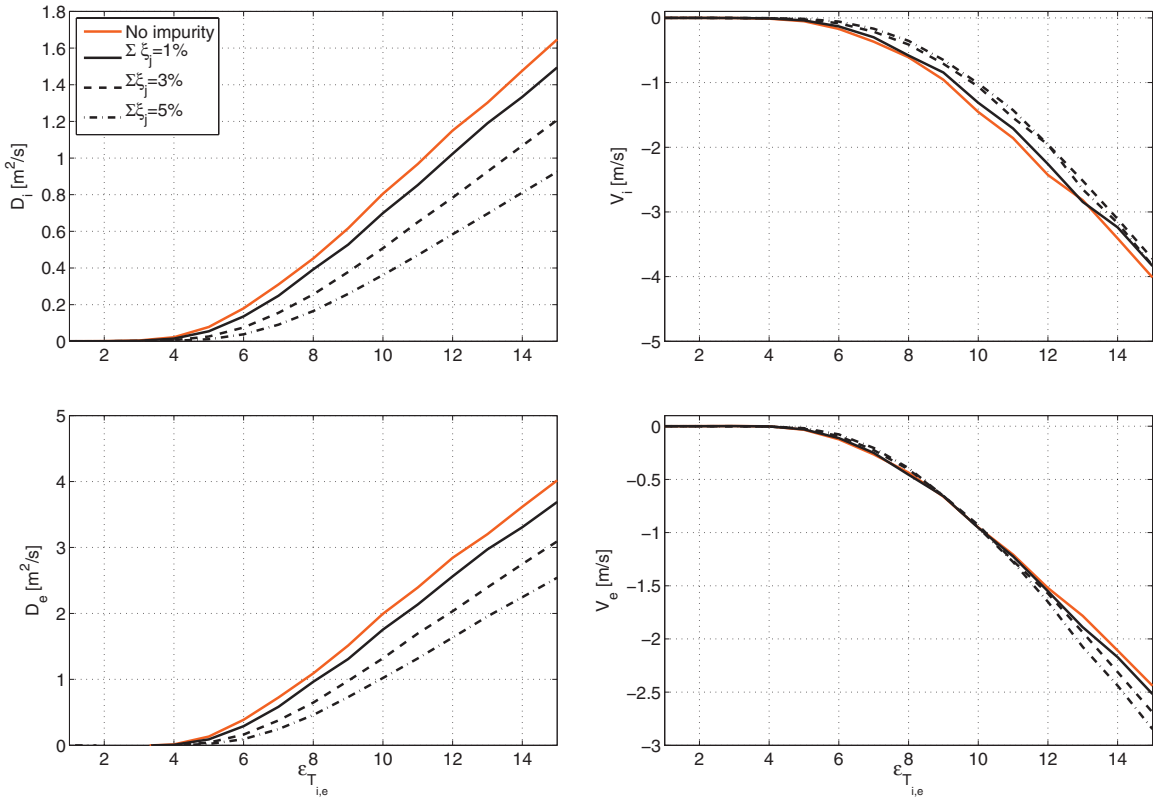

FIG. 6. (Color) Diffusivity and pinch velocity of deuterons and electrons, $D_{i,e}$ (left column) and $V_{i,e}$ (right column), respectively, vs $\epsilon_{T_{e,i}}$ calculated for $s=1.8$.

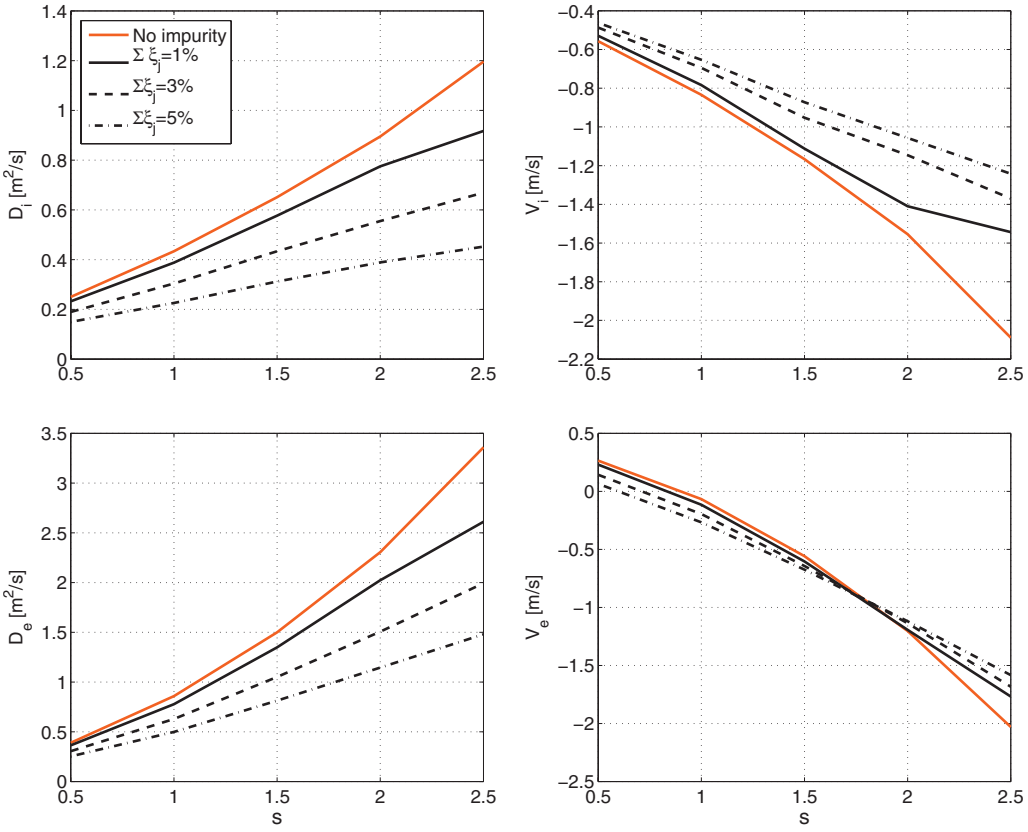

FIG. 7. (Color) Diffusivity and pinch velocity of deuterons and electrons vs magnetic shear calculated for $\epsilon_{T_{e,i}}=10$.

$$q_{e,j} = -\kappa_{e,j}\frac{\partial T_{e,j}}{\partial r} + \Pi_{e,j}T_{e,j},$$

with the heat conduction and pinch factors,

$$\kappa_{e,j} = -\frac{T_e k_y R}{eB}|\tilde{\varphi}|^2 \mathrm{Im}\, Q^{\nabla T}_{et,j},$$

$$\Pi_{e,j} = -\frac{2T_e k_y}{eB}|\tilde{\varphi}|^2 \mathrm{Im}\, Q^{T}_{et,j}. \quad (17)$$

Figures 10 and 11 show the calculated $\kappa_{e,j}$ and $\Pi_{i,e}$ as functions of $\epsilon_{T_e}=\epsilon_{T_i}$ and magnetic shear, respectively. These transport coefficients also reduce with increasing impurity concentration. The heat pinch factor for electrons exhibits a change in sign by varying both the temperature gradient scale and the magnetic shear. The absolute value of Π_e can decrease significantly by increasing impurity concentration. This behavior together with the reduction of the heat diffusivity can contribute noticeably to the reduction of the total heat transport observed in experiments with deliberate impurity seeding.[5] Finally note that both Figs. 7 and 11 show an increase of transport with magnetic shear, although the growth rate of the dominating mode is decreasing with s, see Fig. 5, left column. This is because the wave number of these modes decreases with s even stronger, see Fig. 5, right column, and in the mixing length approximation used above $|\tilde{\varphi}| \sim k_y^{-2}$.

V. CONCLUSION

An approach to model drift instabilities in fusion plasma, containing impurity at high enough concentration, is proposed. The effects of impurities are taken into account in an iterative procedure and arbitrary number of impurity species can be included into consideration. Calculations for deuterium plasmas with Ne^{+10} impurity ions show that the results obtained with the new approach reproduce well those found by taking explicitly one impurity species into account. The found characteristics of unstable modes are sensitive to the concentration and density gradient of impurity. In realistic plasmas with several impurity ion species, the latter are often characterized by very different peaking factors. Therefore an introduction of an effective impurity ion is very uncertain and the present method, which can take into account individually all present impurity species, provides an advantage by considering the impact of impurities on anomalous transport in fusion plasmas. As an example the effects of impurity on ion temperature and trapped electron instabilities in plasmas with several impurity ions including C^{+6}, N^{+7}, O^{+8}, Ne^{+10}, and Ar^{+18} have been studied, with the density

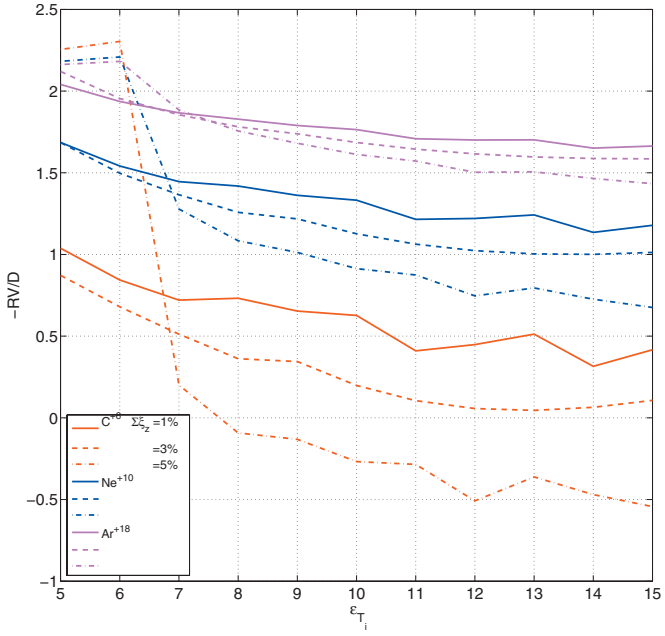

FIG. 8. (Color) The peaking factor for impurity species C^{+6} (red curves), Ne^{+10} (blue curves), and Ar^{+18} (pink curves) vs ϵ_{T_i} computed with $\epsilon_{T_e}=0$, $s=1.8$, and different total impurity concentrations: $\Sigma\xi_j=1\%$ (solid curves), 3% (dashed curves), and 5% (dashed-dotted curves).

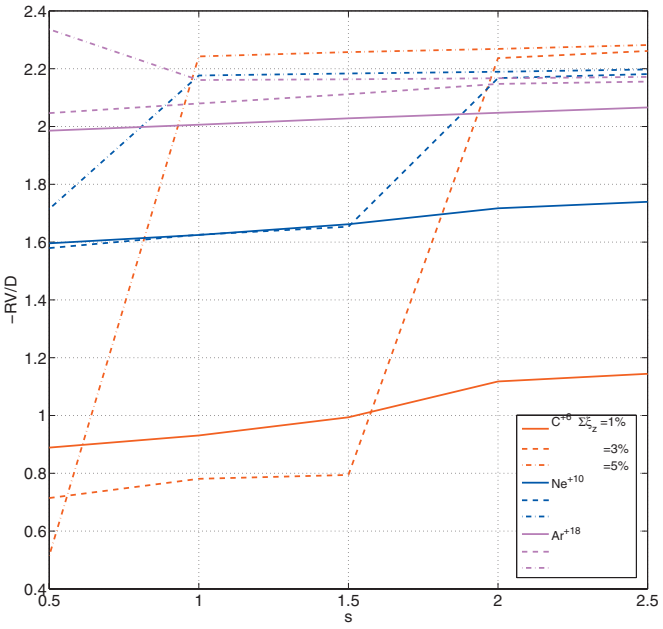

FIG. 9. (Color) The peaking factor for impurity species C^{+6} (red curves), Ne^{+10} (blue curves), and Ar^{+18} (pink curves) vs magnetic shear computed with $\epsilon_{T_e}=0$, $\epsilon_{T_i}=5$, and different total impurity concentrations: $\Sigma\xi_j=1\%$ (solid curves), 3% (dashed curves), and 5% (dashed-dotted curves).

peaking factors determined self-consistently from the condition of zero particle flux. This consideration shows the significant effect of impurities on the anomalous transport of charged particles and heat due to ITG/TE unstable modes.

ACKNOWLEDGMENTS

This work, supported by the European Communities under the contract of Association between EURATOM and the Belgian State, was carried out within the framework of the European Fusion Development Agreement. The views and opinions expressed herein do not necessarily reflect those of the European Commission. S.M. acknowledges FNRS-FRIA of Belgium for financial support.

APPENDIX: PARTICLE AND HEAT FLUX

The density of anomalous particle flux is given, see also Ref. 16, by

$$\Gamma_j = v_\perp \delta n_j^* + v_\perp^* \delta n_j, \tag{A1}$$

where $v_\perp = (\mathbf{E}\times\mathbf{B}/B^2) = -i(k_y/B)\delta\varphi$; the perturbation of particle density is related to that of electrostatic potential, $\delta n_j/n_j = P_j\tilde{\varphi}$, through the coefficients P_j which follow from Eqs. (8)–(10) for ion species and Eqs. (11) and (12) for trapped electrons:

$$P_j = P_{D_j}\epsilon_{n_j} + P_{V_j}, \tag{A2}$$

with

$$P_{D_j} = N_j^{-1}\left\{\bar{\omega}^2\left[\lambda - \frac{m_j}{Z_j^2 m_i}(\lambda\tau_j)k_\perp^2\rho_s^2\right] - \bar{\omega}\left[\frac{1}{3}\frac{\lambda^2\tau_j}{Z_j} - \frac{1}{3}\frac{m_j}{Z_j^3 m_i}(\lambda\tau_j)^2 k_\perp^2\rho_s^2\right] - \left[\frac{15}{3}\lambda\left(\frac{\lambda\tau_j}{Z_j}\right)^2 + \frac{10}{3}\frac{m_j}{Z_j^4 m_i}(\lambda\tau_j)^3 k_\perp^2\rho_s^2 - \frac{2}{3}\xi\frac{m_i}{m_j}\lambda\tau_j\right]\right\}, \tag{A3}$$

$$P_{V_j} = N_j^{-1}\left\{\bar{\omega}^3\left[-\frac{m_j}{Z_j m_i}k_\perp^2\rho_s^2\right] + \bar{\omega}^2\left[-\frac{m_j}{Z_j^2 m_i}(\lambda\tau_j)k_\perp^2\rho_s^2\left(\epsilon_{T_j} - \frac{1}{3}\right)\right] + \bar{\omega}\left[-\frac{m_j}{Z_j^3 m_i}(\lambda\tau_j)^2 k_\perp^2\rho_s^2\left(-\frac{1}{3}\epsilon_{T_j} - \frac{10}{3}\right) - \lambda\left(\frac{\lambda\tau_j}{Z_j}\right)\epsilon_{T_j} + \xi\frac{m_i}{m_j}\tau_j\right] + \left[-\frac{m_j}{Z_j^4 m_i}(\lambda\tau_j)^3 k_\perp^2\rho_s^2\left(-\frac{10}{3}\epsilon_{T_j}\right) + 2\lambda\left(\frac{\lambda\tau_j}{Z_j}\right)^2\epsilon_{T_j} + \xi\frac{m_i}{m_j}\tau_j\left(\frac{5}{3}\frac{\lambda\tau_j}{Z_j} + \lambda\epsilon_{T_j}\right)\right]\right\}, \tag{A4}$$

and

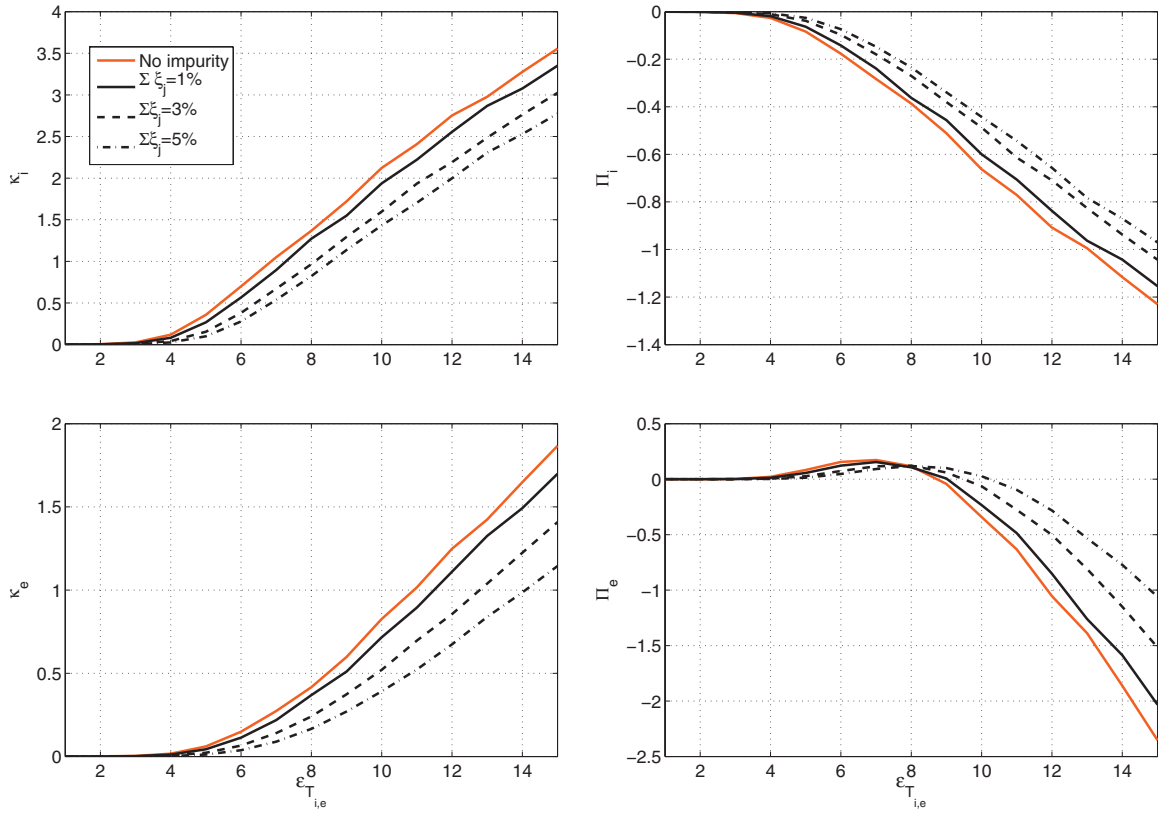

FIG. 10. (Color) Heat transport coefficients $\kappa_{i,e}$ (left column) and $\Pi_{i,e}$ (right column) as functions of $\epsilon_{T_{i,e}}$ calculated for $s=1.8$.

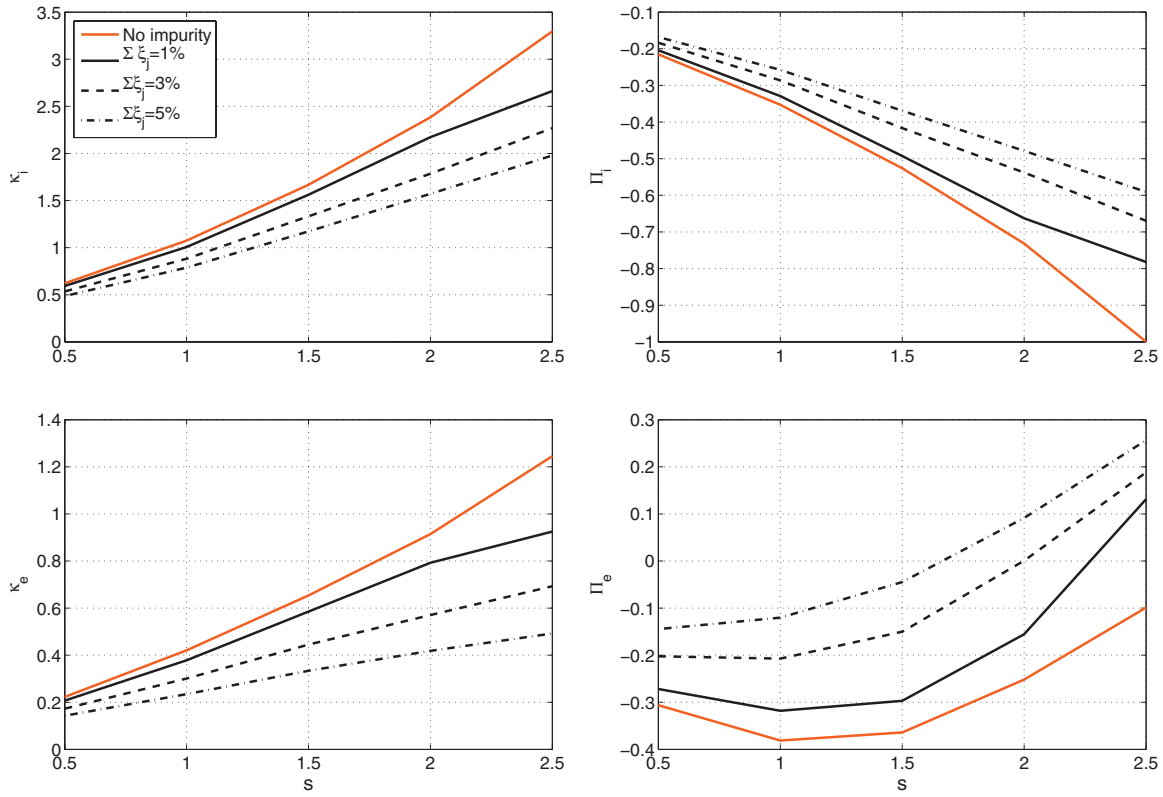

FIG. 11. (Color) Heat transport coefficients vs magnetic shear calculated for $\epsilon_{T_{e,i}}=10$.

$$N_j = \bar{\omega}^3 + \bar{\omega}^2\left[\frac{4}{3}\frac{\lambda\tau_j}{Z_j}\right] - \bar{\omega}\left[\frac{15}{3}\left(\frac{\lambda\tau_j}{Z_j}\right)^2 + \frac{5}{3}\xi\frac{m_i}{m_j}\tau_j\right] - \left[\frac{10}{3}\left(\frac{\lambda\tau_j}{Z_j}\right)^3 + \frac{5}{3}\xi\frac{m_i}{m_j}\tau_j^2\frac{\lambda}{Z_j}\right] - \left[\frac{10}{3}\left(\frac{\lambda\tau_j}{Z_j}\right)^3 + \frac{5}{3}\xi\frac{m_i}{m_j}\tau_j^2\frac{\lambda}{Z_j}\right]. \quad \text{(A5)}$$

As a result one gets

$$\Gamma_j = -2n_j\left|\frac{e\delta\varphi}{T_e}\right|^2\frac{T_e k_y}{eB}\mathrm{Im}(P_j), \quad \text{(A6)}$$

where a mixing length approximation for the potential perturbation amplitude,[16] $e\delta\varphi/T_e \sim \gamma_{\max}/(k_y^2\rho_s c_s)$, is usually used for rough quantitative estimates.

The density of anomalous heat flux can be assessed as[16]

$$q_j = v_\perp\delta(n_jT_j)^* + v_\perp^*\delta(n_jT_j). \quad \text{(A7)}$$

For the q_j part nonvanishing for zero particle flux we get Eq. (16) with the factor Q_j relating the temperature and potential perturbations,

$$Q_j = Q_j^{\nabla T}\epsilon_{T_j} + Q_j^T, \quad \text{(A8)}$$

where

$$Q_j^{\nabla T} = \frac{M_j}{N_j}\left\{\lambda + \frac{2}{3}\bar{\omega}^3\left[-\frac{m_j}{Z_j^2m_i}(\lambda\tau_j)k_\perp^2\rho_s^2\right] + \frac{2}{3}\bar{\omega}^2\left[\frac{1}{3}\frac{m_j}{Z_j^3m_i}(\lambda\tau_j)^2k_\perp^2\rho_s^2 - \lambda\left(\frac{\lambda\tau_j}{Z_j}\right)\right] + \frac{2}{3}\bar{\omega}\left[\frac{10}{3}\frac{m_j}{Z_j^4m_i}(\lambda\tau_j)^3k_\perp^2\rho_s^2 + 2\lambda\left(\frac{\lambda\tau_j}{Z_j}\right)^2 + \xi\frac{m_i}{m_j}\tau_j\lambda\right]\right\}, \quad \text{(A9)}$$

$$Q_j^T = \frac{M_j}{N_j}\left\{\left[-\frac{2}{3}\lambda + \frac{2}{3}\bar{\omega}P_{D_j}N_j\right]\epsilon_{n_j} + \frac{2}{3}\bar{\omega}^4\left[-\frac{m_j}{Z_jm_i}k_\perp^2\rho_s^2\right] + \frac{2}{3}\bar{\omega}^3\left[\frac{1}{3}\frac{m_j}{Z_j^2m_i}(\lambda\tau_j)k_\perp^2\rho_s^2\right] + \frac{2}{3}\bar{\omega}^2\left[\frac{10}{3}\frac{m_j}{Z_j^3m_i}(\lambda\tau_j)^2k_\perp^2\rho_s^2 + \xi\frac{m_i}{m_j}\tau_j\right] + \frac{2}{3}\bar{\omega}\left[\frac{5}{3}\xi\frac{m_i}{m_j}\tau_j\left(\frac{\lambda\tau_j}{Z_j}\right)\right]\right\}, \quad \text{(A10)}$$

where $M_j = \bar{\omega} + (5/3)(\lambda\tau_j/Z_j)$.

[1] E. A. Lazarus, J. D. Bell, C. E. Bush, A. Carnevali, J. L. Dunlap, P. H. Edmonds, L. C. Emerson, O. C. Eldridge, W. L. Gardner, H. C. Howe, D. P. Hutchinson, R. R. Kindsfather, R. C. Isler, R. A. Langley, C. H. Ma, P. K. Mioduszewski, M. Murakami, L. E. Murray, G. H. Neilson, V. K. Parff, S. D. Scott, D. J. Sigmara, J. E. Simpkins, K. A. Stewart, C. E. Thomas, R. M. Wieland, J. B. Wilgen, A. L. Wintenberg, W. R. Wing, and A. J. Wootton, J. Nucl. Mater. **121**, 61 (1984).

[2] J. Ongena, R. Budny, P. Dumortier, G. L. Jackson, H. Kubo, A. M. Messiaen, M. Murakami, J. D. Strachan, R. Sydora, M. Tokar, B. Unterberg, U. Samm, P. E. Vandenplas, R. Weynants, N. Asakura, M. Brix, M. Charlet, I. Coffey, G. Cordey, S. K. Erents, G. Fuchs, M. von Hellermann, D. L. Hillis, J. Hogan, L. D. Horton, L. C. Ingesson, K. Itami, S. Jachmich, A. Kallenbach, H. R. Koslowski, A. Kraemer-Flecken, K. D. Lawson, A. Loarte, G. P. Maddison, G. Mank, G. R. McKee, A. Meigs, F. Milani, P. Monier-Garbet, M. F. F. Nave, M. E. Puiatti, V. Parail, J. Rapp, S. Sakurai, S. Sharapov, F. Sartori, M. Stamp, H. Tamai, G. Telesca, M. Valisa, G. Van Wassenhove, B. Weyssow, and K.-D. Zastrow, Phys. Plasmas **8**, 2188 (2001).

[3] H. Kubo, S. Sakurai, N. Asakura, S. Konoshima, H. Tamai, S. Higashijima, A. Sakasai, H. Takenaga, K. Itami, K. Shimizu, T. Fujita, Y. Kamada, Y. Koide, H. Shirai, T. Sugie, T. Nakano, N. Oyama, H. Urano, T. Ishijima, K. W. Hill, D. R. Ernst, A. W. Leonard, and JT-60 Team, Nucl. Fusion **41** 227 (2001).

[4] G. F. Matthews, B. Balet, J. G. Cordey, S. J. Davies, G. M. Fishpool, H. Y. Guo, L. D. Horton, M. G. von Hellermann, L. C. Ingesson, J. Lingertat, A. Loarte, G. M. McCracken, C. F. Maggi, R. D. Monk, V. V. Parail, R. Reichle, M. F. Stamp, P. C. Stangeby, D. Stork, A. Taroni, G. C. Vlases, and K.-D. Zastrow, Nucl. Fusion **39**, 19 (1999).

[5] X. Litaudon, G. Arnoux, M. Beurskens, S. Brezinsek, C. D. Challis, F. Crisanti, P. C. DeVries, C. Giroud, R. A. Pitts, F. G. Rimini, Y. Andrew, M. Ariola, Y. F. Baranov, M. Brix, P. Buratti, R. Cesario, Y. Corre, E. De La Luna, W. Fundamenski, E. Giovannozzi, M. P. Gryaznevich, N. C. Hawkes, J. Hobirk, A. Huber, S. Jachmich, E. Joffrin, H. R. Koslowski, Y. Liang, Th. Loarer, P. Lomas, T. Luce, J. Mailloux, G. F. Matthews, D. Mazon, K. McCormick, D. Moreau, V. Pericoli, V. Philipps, E. Rachlew, S. D. A. Reyes-Cortes, G. Saibene, S. E. Sharapov, I. Voitsekovitch, L. Zabeo, O. Zimmermann, K. D. Zastrow, and JET-EFDA Contributors, Plasma Phys. Controlled Fusion **49**, B529 (2007).

[6] R. Paccagnella, F. Romanelli, and S. Briguglio, Nucl. Fusion **30**, 545 (1990).

[7] M. Frojdh, M. Liljestrom, and H. Nordman, Nucl. Fusion **32**, 419 (1992).

[8] R. R. Dominguez and G. M. Staebler, Nucl. Fusion **33**, 51 (1993).

[9] M. Z. Tokar, R. Jaspers, R. R. Weynants, H. R. Koslowski, A. Krämer-Flecken, A. M. Messiaen, J. Ongena, and B. Unterberg, Plasma Phys. Controlled Fusion **41**, L9 (1999).

[10] T. Fülöp and J. Weiland, Phys. Plasmas **13**, 112504 (2006).

[11] H. Nordman and T. Fülop, Phys. Plasmas **14**, 052303 (2007).

[12] T. Fülöp and H. Nordman, Phys. Plasmas **16**, 032306 (2009).

[13] C. Giroud, C. Angioni, G. Bonheure, I. Coffey, N. Dubuit, X. Garbet, R. Guirlet, P. Mantica, V. Naulin, M. E. Puiatti, M. Valisa, A. D. Whiteford, K.-D. Zastrow, M. N. A. Beurskens, M. Brix, E. de la Luna, K. Lawson, L. Lauro-Taroni, A. Meigs, M. OMullane, T. Parisot, C. Perez Von Thun, O. Zimmermann, and JET-EFDA Contributors, "Progress in understanding impurity transport at JET," FEC 2006, Chengdu, Paper No. EX/8-3, 2006.

[14] C. Angioni and A. G. Peeters, Phys. Rev. Lett. **96**, 095003 (2006).

[15] S. Moradi, M. Z. Tokar, R. Singh, and B. Weyssow, Nucl. Fusion **49**, 085007 (2009).

[16] J. Weiland, *Collective Modes in Inhomogeneous Plasmas: Kinetic and Advanced Fluid Theory* (Institute of Physics, Bristol, 2000).

[17] S. I. Braginskii, Rev. Plasma Phys. **1**, 205 (1965).

[18] J. Nilsson and J. Weiland, Nucl. Fusion **34**, 803 (1994).

[19] H. Nordman, P. Strand, and G. Garbet, Plasma Phys. Controlled Fusion **49**, 985 (2007).

[20] A. Hirose, L. Zhang, and M. Elia, Phys. Plasmas **2**, 859 (1995).

[21] C. Giroud, C. Angioni, L. Carraro, I. H. Coffey, J. Hobirk, M. E. Puiatti, M. Valisa, A. D. Whiteford, P. Belo, T. M. Biewer, M. Brix, R. Buttery, E. Joffrin, L. Lauro Taroni, K. Lawson, P. Mantica, A. Meigs, V. Naulin, M. G. O'Mullane, K.-D. Zastrow, and JET-EFDA Contributors, "Study of Z dependence of impurity transport at JET," Proceedings of the 34th EPS on Plasma Physics, Warsaw, Poland 2007.